

Molecular Weight Dependence of Polymer Chain Mobility within Multilayer Films

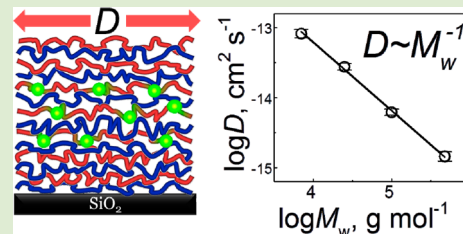
Li Xu,[†] Victor Selin,[†] Aliaksandr Zhuk,[†] John F. Ankner,[‡] and Svetlana A. Sukhishvili^{*,†}

[†]Department of Chemistry, Chemical Biology and Biomedical Engineering, Stevens Institute of Technology, Hoboken, New Jersey 07030, United States

[‡]Spallation Neutron Source, Oak Ridge National Laboratory, Oak Ridge, Tennessee 37831, United States

Supporting Information

ABSTRACT: Fluorescence recovery after photobleaching has been applied to determine, to our knowledge for the first time, the molecular weight (M_w) dependence of lateral diffusion of polymer chains within layer-by-layer (LbL) films. As shown by neutron reflectometry, polyelectrolyte multilayers containing polymethacrylic acid (PMAA, $M_w/M_n < 1.05$) of various molecular weights assembled from solutions of low ionic strengths at pH 4.5, where film growth was linear, showed similar diffusion of PMAA in the direction perpendicular to the film surface. At a salt concentration sufficient for unfreezing electrostatically bonded chains, layer intermixing remained almost unaffected (changes < 1.0 nm), while the lateral diffusion coefficient (D) scaled with the PMAA molecular weight as $D \sim M_w^{-1+0.05}$.



Polyelectrolyte multilayers (PEMs)¹ are multicomponent materials with promising applications for enhanced photoluminescence,² improved antireflection coatings,³ or multistage delivery of therapeutic compounds from surfaces.⁴ Many of these applications rely on internal film layering, resulting from the inherently nonequilibrium nature of these films. Indeed, films whose thickness increases linearly with the polyelectrolyte (PE) adsorption cycle during layer-by-layer (LbL) deposition usually have a layered internal structure, arising from multisite, strong sequential adsorption of polymer chains. In the case of weak interpolyelectrolyte interactions, however, chain intermixing can occur during film deposition⁵ or postassembly.^{6–8} Significant chain mobility can be induced in strongly bound, stratified PEMs by addition of salt and monitored by atomic force microscopy (AFM),⁶ fluorescence recovery after photobleaching (FRAP),^{7,8} or neutron reflectometry (NR).^{10–12} Understanding the factors affecting molecular motions within PEM films is critical for potential applications of these films that rely on internal film structuring.

Apart from ionic strength, the mobility of polymer chains within multilayer films is also affected by solution pH,^{13,14} type of salt,⁷ and temperature,^{7,9} as well as properties of polymer chains, such as charge density, chain rigidity, hydrophobicity,^{7,9} and steric bulk at charged units.¹² Paradoxically, the effect of another fundamental parameter—polymer molecular weight—on chain mobility within PEM films is much less understood.^{13–16} In our earlier work, we have explored molecular weight dependence of the release rate of polyelectrolytes from PEMs induced by pH changes.¹⁴ Very recently, Char and co-workers also reported that changes of film internal structure and the disintegration mode of PEM films in response to pH changes were dependent on the PE molecular weight.¹⁵ An interesting counterintuitive dependence of the vertical diffusion

of a polyanion on a polycation molecular weight has been recently found by Helm and co-workers.¹⁶ No experiments have been yet carried out, to the best of our knowledge, to probe molecular weight dependence of lateral motions of polymer chains within PEMs.

Lack of knowledge of the fundamental laws behind motions of polymer chains assembled within PEM films is in strong contrast with the abundant literature on polymer diffusion in melts,¹⁷ dilute solutions,¹⁸ and even the less understood, more recently studied diffusion of polymers at the solid–liquid interface.¹⁹ This communication aims to fill this gap by reporting experiments to quantitatively access the role of PE molecular weight on lateral chain mobility within PEM films. By applying the fluorescence recovery after photobleaching (FRAP) technique to stratified LbL films assembled with PEs of varied molecular weights and low polydispersity indices (PDIs), we have determined that the center-of-mass diffusion coefficient of PE chains in the direction parallel to the substrate, D_{\parallel} , scales with the inverse of the polymer molecular weight. By applying neutron reflectometry (NR) techniques to the same PEM systems exposed to the same solutions, we found that during significant displacement in the lateral direction chain motion in the direction perpendicular to the surface was much more sluggish, suggesting persistent film layering during annealing in salt solutions.

PEM films were constructed using poly(2-(dimethylamino)-ethyl methacrylate) as a polycation (PC, M_w 30 kDa, $M_w/M_n \approx 1.10$) and polymethacrylic acid (PMAA) with M_w/M_n 1.02–1.05 of various molecular weights. PC was synthesized by atom

Received: August 6, 2013

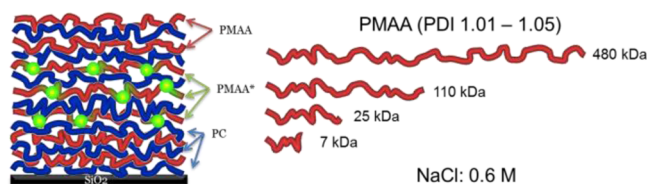
Accepted: September 12, 2013

Published: September 16, 2013

transfer radical polymerization (ATRP) (see Supporting Information for detailed procedures), whereas PMAA with $M_w = 7$, 25, and 110 kDa abbreviated as PMAA_{7k}, PMAA_{25k}, and PMAA_{110k}, respectively, was purchased from Polymer Source, Inc. PMAA with M_w 480 kDa denoted as PMAA_{480k} was purchased from Polymer Standards Service, Inc. For all PMAA molecular weights, PC/PMAA films, deposited by dipping using 0.2 mg/mL polymer solutions in 0.01 M phosphate buffer at pH 4.5, showed linear film growth as measured by ellipsometry (Figure S1, Supporting Information). At this pH, assembled PMAA of all molecular weights was $26 \pm 2\%$ ionized, as determined by FTIR of dry 50-bilayer films deposited on IR-transparent silicon wafers (Figure S2, Supporting Information) following a procedure described in our earlier paper.²⁰ Assembly of PC/PMAA films at pH > 5.5 results in exponential rather than linear film growth.²¹ Therefore, in this letter we have chosen to explore films deposited at pH = 4.5, where films are layered. The ellipsometric bilayer thickness of dry PC/PMAA films increased by $\sim 30\%$ from ~ 2.5 to ~ 3.3 nm as the molecular weight of PMAA used for the film construction increased from 7 to 110 and 480 kDa, with intermediate bilayer thicknesses for films constructed with PMAA_{25k} (Table S1, Supporting Information). This increase is small compared to an ~ 4 -fold difference in the size of unbound PMAA chains. The dimensions of unbound polymer chains were estimated as $2R_G$ (where R_G is the radius of gyration of a polymer coil) using the Gaussian approximation and adopting the value of monomer length and the persistence length (L_p) of PMAA chains as 0.255 and 0.3 nm, respectively.²² The calculated $2R_G$ values were 3, 5.5, 12, and 25 nm for PMAA_{7k}, PMAA_{25k}, PMAA_{110k}, and PMAA_{480k} respectively. Obviously, PMAA chains of all molecular weights adopt a “flat” conformation within PEM films. The chain “flattening” occurs due to strong, cooperative binding of PMAA with highly charged PC chains at pH 4.5 (pK_a of poly(2-(dimethylamino)ethyl methacrylate) is ≈ 6.7).²³ A very weak dependence of the adsorption amount on the polyelectrolyte degree of polymerization has also been found for other strongly bound LbL systems.²⁴

Scheme 1 shows the architecture of the PEM films used in the FRAP measurements. PMAA was tagged with an Alexa

Scheme 1. Schematic Representation of Multilayers Used in Measurements of Diffusion Coefficients of PMAA Chains within PEM Films in FRAP Experiments



Fluor 488 molecule every 300th monomer unit to yield PMAA*. FRAP experiments were performed with a custom-made setup using a 488 nm excitation Stabilite 2017 laser (Spectra-Physics) and a PerkinElmer SPCM-AQR photon counter using 1 mW laser power for bleaching and 1 μ W for detecting fluorescence recovery (see Supporting Information for complete procedures). Fluorescently tagged PMAA* layers were assembled within the central region of the LbL film (Scheme 1), to avoid effects of the solid surface and polymer–water interface on polymer dynamics and film structure. In our

prior report, we found that “sandwiching” PMAA* in between two unlabeled PC/PMAA bilayers deposited within the substrate and upper regions of the film was sufficient to confine marker layers within the film center.²⁵ Control experiments with a single PMAA* marker layer showed that PMAA* diffusion within the middle region of the film was independent of the layer position (chain mobility was consistent within 10%). For improved sensitivity, however, here we present data taken with three PMAA* marker layers included in the middle region of the films.

Layered PEMs are strongly bound by a network of ionic pairing that inhibits PE chain diffusion in the absence of salts. Consistent with this general observation, the fluorescence intensity of the bleached spot did not recover for PEM samples at all PMAA molecular weights, when bleached films were exposed to 0.01 M phosphate buffer with no additional salt (data not shown). Small ions screen electrostatic interactions, compete with ionic pairing, and lower the potential barrier for polymer chain diffusion. As in other reports,^{7–11,25} we have used salt to induce polyelectrolyte chain motion within PEM films. Figure 1 shows that PMAA molecular weight strongly

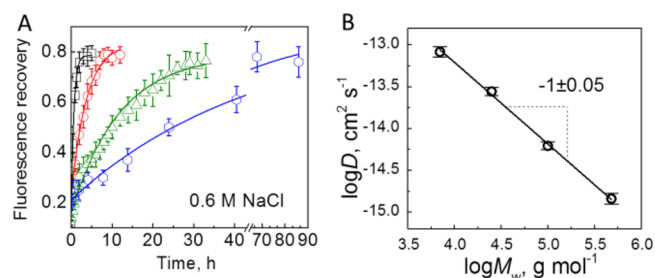


Figure 1. FRAP recovery curves obtained with (PC/PMAA)₂/(PC/PMAA*)₃/(PC/PMAA)₂ PEMs containing PMAA* of various molecular weights, exposed to 0.6 M NaCl solutions at pH 4.5 (A). Multilayer films were constructed using PMAA_{7k} (squares), PMAA_{25k} (circles), PMAA_{110k} (triangles), PMAA_{480k} (hexagons), and corresponding PMAA* with the same molecular weights. (B) Log–log plots of lateral diffusion coefficients, D_{\parallel} , versus PMAA (PMAA*) molecular weight.

affected chain diffusion in salt solutions. After annealing in salt solutions, the fluorescence intensity of the bleached spot recovered to $\sim 80\%$ of the original value. Incomplete recovery of the bleached spot is possibly due to partial cross-linking of PC/PMAA films upon exposure to the 1 mW bleaching beam. As expected, high ionic strengths and low PMAA molecular weights favored faster chain mobility. Note that our choice of salt concentration was dictated by the instability to decomposition of the film with the shortest PMAA (PMAA_{7k}) at 0.8 M NaCl, whereas films with the longest PMAA chains (PMAA_{480k}) diffuse in 0.4 M NaCl solutions (data not shown) too slowly for experimental convenience. The data in Figure 1A could be fitted by a single exponential function, with a characteristic half time for fluorescence recovery $t_{1/2}$. The lateral diffusion coefficients D_{\parallel} of PEM-assembled PMAA* were then calculated as $D_{\parallel} = \gamma R^2 / 4t_{1/2}$ (where $\gamma = 1.4$ for the spherical beam spot with a Gaussian intensity distribution,²⁶ and $R = 0.205 \mu\text{m}$ is the radius of the bleaching spot). The data for D_{\parallel} were measured repeatedly at different points on the same multilayer films and with different samples (new cells, new PC/PMAA films). For the measured PMAA molecular weights, D_{\parallel} was in the range 10^{-14} – 10^{-15}

cm^2/s . For example, D_{\parallel} of PMAA* decreased from $(8.26 \pm 0.15) \times 10^{-14}$ to $(6.20 \pm 1.00) \times 10^{-15}$ cm^2/s between PMAA_{7k} and PMAA_{110k} for PC/PMAA films upon exposure to 0.6 M NaCl solutions. Table S2 (Supporting Information) summarizes the values of D_{\parallel} for all systems.

Figure 1B shows that the relationship between lateral diffusion D_{\parallel} and molecular weight M_w of diffusing PMAA* within PC/PMAA PEMs upon exposure to 0.6 M NaCl solutions follows a power law with exponent -1.00 ± 0.05 . The data for lateral diffusion revealed $D_{\parallel} \sim M_w^{-1}$ with $\pm 10\%$ variation. The key question is how to understand the diffusion law. Dynamical transport scenarios are diverse and dependent on the conformation of assembled polyelectrolyte chains. We therefore need also to measure the effect of PMAA molecular weight and solution ionic strength on chain intermixing in the direction *perpendicular* to the substrate. To probe the quality of film layering using NR, marker layers of deuterated PMAA (dPMAA) with molecular weights 5, 40, and 180 kDa (dPMAA_{5k}, dPMAA_{40k}, and dPMAA_{180k}, PDI < 1.1, Polymer Source, Inc.) were assembled as every fifth bilayer within PC/PMAA_{7k}, PC/PMAA_{25k}, and PC/PMAA_{110k} PEMs, respectively. Figure 2 and Figure S3 (Supporting Information) show NR

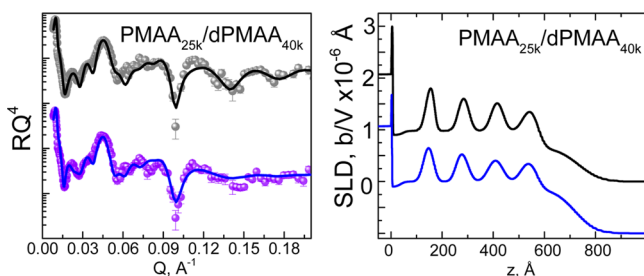


Figure 2. Neutron reflectivity data (plotted as $R \times Q^4$ to enhance small features) (left) and corresponding fitted scattering length density profiles (right) for dry [(PC/PMAA_{25k})₄/(PC/dPMAA_{40k})₄]/(PC/PMAA_{25k})₄ PEM samples after annealing for 54 h in 0.01 M phosphate buffer with no salt and in 0.6 M NaCl solutions (indicated as black and colored lines and symbols, respectively). For clarity, the data for annealed samples were shifted down by 10^{-2} (left) and 10^{-6} (right) along the vertical axis.

data (left) and the fitted scattering length density profiles (right) for 24-bilayer PC/PMAA films after exposure to buffer solutions with no additional salt ('no-salt') or with additional 0.6 M NaCl for 54 h. Bragg peaks indicate layering within the PEMs, but the polymers are significantly intermixed within the LbL films (see structural parameters in Tables S3–S8, Supporting Information). The thickness of the dPMAA marker layers increased ~ 15 – 60% between the first and fourth dPMAA marker layers with distance from the substrate due to accumulated interfacial mixing. Tables S3, S5, and S7 in the Supporting Information show that this trend was observed for all PMAA molecular weights, with the shortest PMAA having the highest values of NR internal roughnesses, σ_{int} of dPMAA marker layers. Specifically, the 24-bilayer PC/PMAA_{7k} films showed σ_{int} of 3.5, 4.0, 4.1, and 5.2 nm, starting from the closest-to-the-substrate marker, where the widths are given as full-width-at-half-maximum (fwhm), which is a factor of 2.35 larger than the Gaussian σ_{int} used in some other reports.⁷ This trend was consistent with atomic force microscopy (AFM) measurements of roughness of the dry film–air interface, σ_{air} , giving 3.1, 5.2, 5.9, and 6.1 nm for 5-, 10-, 15-, and 20-bilayer PC/PMAA_{7k} films. To compare films of different PMAA

molecular weights, we have used the thicknesses of the closest-to-the-substrate dPMAA marker layers (d , as shown in Tables S3, S5, and S7, Supporting Information). Importantly, the NR thickness of these layers was almost independent of the PMAA molecular weight and assumed values between 3.3 and 3.8 nm for all film types.

Figure 2 illustrates that annealing in salt solutions (0.6 M NaCl) also had a negligibly small effect on layering within PC/PMAA_{25k} films, resulting in the interfacial roughness change, $\Delta\sigma_{\text{int}}$, less than 0.4 nm for the closest-to-the-substrate dPMAA layer. For films with longer PMAA_{180k}, such annealing resulted in even smaller, 0.1 nm, $\Delta\sigma_{\text{int}}$ values. These subdiffusion lengths yield the upper limit of the PMAA_{40kDa} intermixing rate in the transverse direction, D_{\perp} , of 3.70×10^{-20} cm^2/s , as calculated for the closest-to-substrate dPMAA layer from the equation

$$\Delta\sigma_{\text{int}}^2 = 2D_{\perp}\Delta t$$

(where Δt is the salt annealing time) assuming that diffusion of polymer chains follows a Gaussian distribution. Note that though PEMs with the shortest PMAA_{7k} annealed in 0.6 M NaCl solutions deviated from this model (Figure S3, Supporting Information) FRAP data for PC/PMAA_{7k} films were consistent with the $D \sim M_w^{-1 \pm 0.05}$ scaling. While the lateral chain motions extended to distances larger than the size of polymer coils, motions in the direction perpendicular to the substrate were at least 10^4 -fold slower for all PEM films. PE segments, therefore, are spread over similar distances in the direction perpendicular to the substrate, and film layering for the larger molecular weights is not significantly affected by salt-induced lateral center-of-mass chain motions. While the physical origins of potential barriers to such chain motions are not yet understood, structural templating by the solid surface and inhibited vertical chain motions as a result of adsorption-induced chain flattening are likely candidates.

The central outcome of this work is measuring the molecular weight dependence of PE diffusion. While $D \sim M^{-1}$ formally follows Rouse dynamics, it is obvious that the physical laws behind chain motions within ionic networks must be fundamentally different from the assumptions of the Rouse model. Origins of the $D \sim M^{-1}$ scaling should be related to specific conformations of assembled polymer chains, and answers might be sought in the reversible reorganization of ionic networks with discrete binding sites and free energy barriers to chain motion. While the effects of polyelectrolyte type, chain rigidity, charge density, salt concentration, and the structure of PEM films on the D vs M scaling law are still to be tested, we suggest that our findings should motivate further development of theoretical and experimental insights into the dynamic behavior of layered PEM films.

■ ASSOCIATED CONTENT

📄 Supporting Information

Experimental details for polymer synthesis, sample preparation, and fitting of neutron reflectivity curves. This material is available free of charge via the Internet at <http://pubs.acs.org>.

■ AUTHOR INFORMATION

Corresponding Author

*E-mail: ssukhish@stevens.edu.

Notes

The authors declare no competing financial interest.

■ ACKNOWLEDGMENTS

This work was supported by the National Science Foundation under Award DMR-0906474 (S.S.). Neutron measurements were performed at the Spallation Neutron Source at the Oak Ridge National Laboratory, managed by UT-Battelle, LLC, for the DOE under contract No. DE-AC05-00OR22725.

■ REFERENCES

- (1) *Multilayer Thin Films: Sequential Assembly of Nanocomposite Materials*; Decher, G.; Schlenoff, J., Eds.; Wiley & Sons: New York, 2012.
- (2) Schneider, G.; Decher, G.; Nerambourg, N.; Praho, R.; Werts, M. H. V.; Blanchard-Desce, M. *Nano Lett.* **2006**, *6*, 530.
- (3) Wang, T. C.; Cohen, R. E.; Rubner, M. F. *Adv. Mater.* **2002**, *14*, 1534.
- (4) Wood, K. C.; Chuang, H. F.; Batten, R. D.; Lynn, D. M.; Hammond, P. T. *Proc. Natl. Acad. Sci. U.S.A.* **2006**, *103*, 10207.
- (5) (a) Picart, C.; Mutterer, J.; Richert, L.; Luo, Y.; Prestwich, G. D.; Schaaf, P.; Voegel, J.-C.; Lavallo, P. *Proc. Natl. Acad. Sci. U.S.A.* **2002**, *99*, 12531. (b) Lundin, M.; Blomberg, E.; Tilton, R. D. *Langmuir* **2010**, *26*, 3242. (c) Lavallo, P.; Voegel, J.-C.; Vautier, D.; Senger, B.; Schaaf, P.; Ball, V. *Adv. Mater.* **2011**, *23*, 1191.
- (6) (a) Dubas, S. T.; Schlenoff, J. B. *Langmuir* **2001**, *17*, 7725. (b) McAloney, R. A.; Dudnik, V.; Goh, M. C. *Langmuir* **2003**, *19*, 3947.
- (7) Nazaran, P.; Bosio, V.; Jaeger, W.; Anghel, D. F.; von Klitzing, R. *J. Phys. Chem. B* **2007**, *111*, 8572.
- (8) Jourdainne, L.; Lecuyer, S.; Arntz, Y.; Picart, C.; Schaaf, P.; Senger, B.; Voegel, J.-C.; Lavallo, P.; Charitat, T. *Langmuir* **2008**, *24*, 7842.
- (9) Wong, J. E.; Zastrow, H.; Jaeger, W.; von Klitzing, R. *Langmuir* **2009**, *25*, 14061.
- (10) Jomaa, H. W.; Schlenoff, J. B. *Macromolecules* **2005**, *38*, 8473.
- (11) Soltwedel, O.; Ivanova, O.; Nestler, P.; Müller, M.; Köhler, R.; Helm, C. A. *Macromolecules* **2010**, *43*, 7288.
- (12) Xu, L.; Ankner, J. F.; Sukhishvili, S. A. *Macromolecules* **2011**, *44*, 6518.
- (13) Sun, B.; Jewell, C. M.; Fredin, N. J.; Lynn, D. M. *Langmuir* **2007**, *23*, 8452.
- (14) Kharlampieva, E.; Ankner, J. F.; Rubinstein, M.; Sukhishvili, S. A. *Phys. Rev. Lett.* **2008**, *100*, 128303.
- (15) Jang, Y.; Seo, J.; Akgun, B.; Satija, S.; Char, K. *Macromolecules* **2013**, *46*, 4580.
- (16) Soltwedel, O.; Nestler, P.; Neumann, H.-G.; Paßvogel, M.; Köhler, R.; Helm, C. A. *Macromolecules* **2012**, *45*, 7995.
- (17) Doi, M.; Edwards, S. F. *The Theory of Polymer Dynamics*; Clarendon Press: Oxford, UK, 1986.
- (18) (a) Yuko, K.; Chikako, H. *Polym. Commun* **1984**, *25*, 154. (b) Huber, K.; Bantle, S.; Lutz, P.; Burchard, W. *Macromolecules* **1985**, *18*, 1461. (c) Azuma, R.; Takayama, H. *J. Chem. Phys.* **1999**, *111*, 8666.
- (19) (a) Sukhishvili, S. A.; Chen, Y.; Müller, J. D.; Gratton, E.; Schweizer, K.; Granick, S. *Nature* **2000**, *406*, 146. (b) Zhai, J.; Granick, S. *Macromolecules* **2007**, *40*, 1243. (c) Wong, J. S. S.; Hong, L.; Bae, S. C.; Granick, S. *Macromolecules* **2011**, *44*, 3073.
- (20) Kharlampieva, E.; Sukhishvili, S. A. *Langmuir* **2003**, *19*, 1235.
- (21) Xu, L.; Pristinski, D.; Zhuk, A.; Stoddart, C.; Ankner, J. F.; Sukhishvili, S. A. *Macromolecules* **2012**, *45*, 3892.
- (22) Ortiz, C.; G. Hadziioannou, G. *Macromolecules* **1999**, *32*, 780.
- (23) An, S. W.; Thomas, R. K.; Baines, F. L.; Billingham, N. C.; Armes, S. P.; Penfold, J. *Macromolecules* **1998**, *31*, 7877.
- (24) (a) Lösche, M.; Schmitt, J.; Decher, G.; Bouwman, W. G.; Kjaer, K. *Macromolecules* **1998**, *31*, 8893. (b) Büscher, K.; Graf, K.; Ahrens, H.; Helm, Ch. A. *Langmuir* **2002**, *18*, 3585.
- (25) Xu, L.; Kozlovskaya, V.; Kharlampieva, E.; Ankner, J. F.; Sukhishvili, S. A. *ACS Macro Lett.* **2012**, *1*, 127.
- (26) Axelrod, D.; Koppel, D. E.; Schlessinger, J.; Elson, E.; Webb, B. *Biophys. J.* **1976**, *16*, 1055.